

A Study on the Vibration Modal Testing and Analytical Model Updating of Liquid Rocket Engine of KSLV-II

Jongyoun Park*, Yoonwan Moon**, Sehoon Jung***, Indeuk Kang****

*Korean Aerospace Research Institute

169-84 gwahak-ro Yuseong-gu Daejeon Korea, vision@kari.re.kr

**Korean Aerospace Research Institute, ywmoon@kari.re.kr

169-84 gwahak-ro Yuseong-gu Daejeon Korea

***VMVTech

351 Hwangang-ro Bundang-gu Seongnam-si Gyeonggi-do Korea, sehoon.jung@ymv-tech.com

****VMVTech

351 Hwangang-ro Bundang-gu Seongnam-si Gyeonggi-do Korea, indeuk.kang@ymv-tech.com

Abstract

One of the generalized methods to verify the design frequency of the manufactured hardware and to improve the accuracy of the analytical finite element (FE) model is to identify the dynamic characteristics through the vibration modal testing, and to update the FE model by comparing and correlating the experimental modal parameters with the analytical modal parameters. In this paper, an overview of the process and some results of verifying the dynamic characteristics of the 75-ton class engine of the Korean Space Launch Vehicle II (KSLV-II) and updating its FE models through the correlation between the vibration modal testing results and the analysis results are presented.

1. Introduction

1.1 KSLV-II and its LRE

Korea Space Launch Vehicle II(KSLV-II) is the first self-developed space launch vehicle in Korea capable of putting 1.5 ton multipurpose satellite into low orbit at 600~800 km altitude planned launching into the space in 2021.

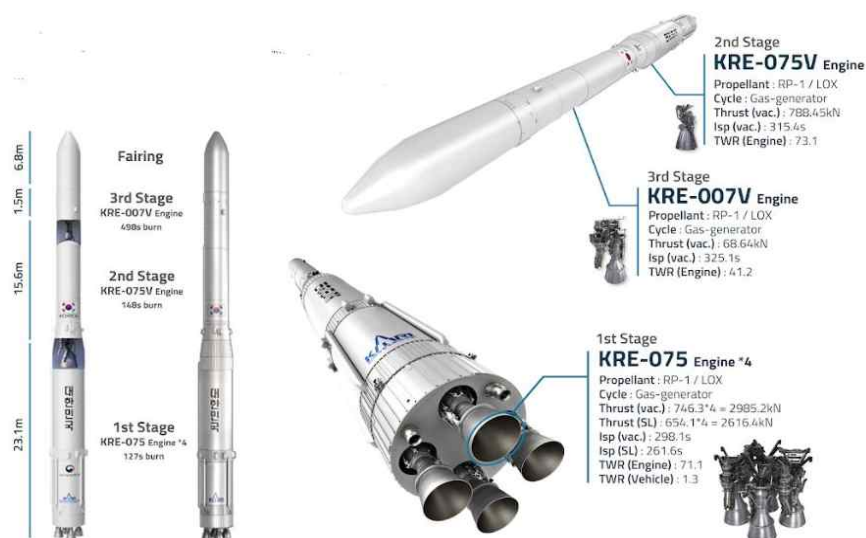


Figure 1: KSLV-II and its LRE

It is a 3-stage launch vehicle that consists of 300 ton 1st stage booster with four 75 ton liquid engines, 2nd stage with one 75 ton liquid engine and 3rd stage with one 7 ton liquid engine. 7 ton and 75 ton engines and their infrastructures such as engine assembly facilities and engine firing test facilities have been developed simultaneously since 2010. The first 7 ton engine was assembled in May 2015 and its first firing test was conducted in July 2015. In March 2016, the first 75 ton engine was assembled and its first test was conducted in May 2016. A number of engine assemblies and firing tests have been carried out since then, and the overall performance of the 75 ton engine was verified through the successful launch of the test launch vehicle (TLV) at Naro Space Center in November 2018.

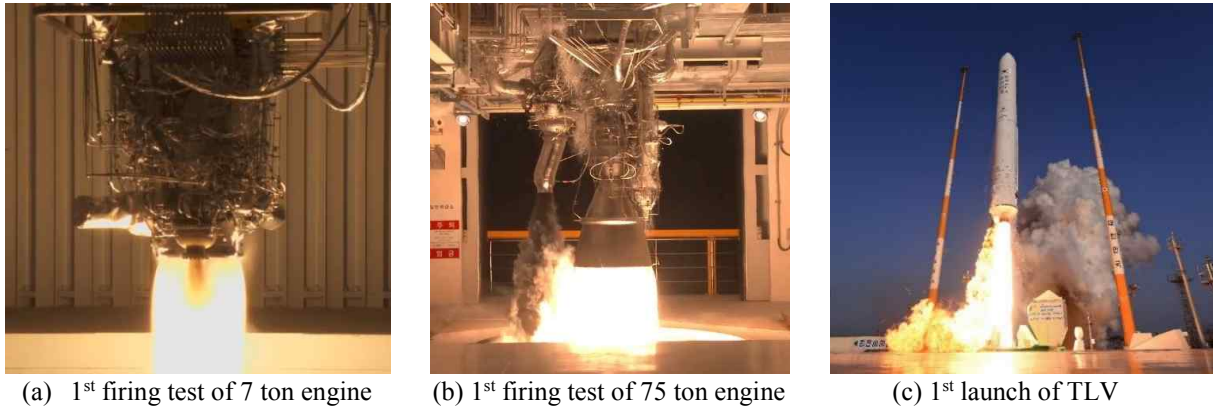


Figure 2: Status of KSLV-II engine development

1.3 Purpose of the research

The modal testing of a structure is the experimental method to determine its dynamic characteristics (or modal parameters) such as natural frequencies, mode shapes, modal dampings, and to provide these characteristics to update the FE model of the structure by correlating the experimental and analytical data.

When developing a liquid rocket engine, the engine and its components have to be developed to avoid coupling with dynamic excitation during launch or operation. The modal testing is the way to demonstrate that the engine conforms to the design frequency requirements. It is also important to validate the engine design through the structural analysis before the manufacturing, assembly and firing test in that it can reduce trial and error at the early stage of the engine design. Since the validation of the design through structural analysis assumes that the reliability of the FE model is guaranteed, making an accurate FE model by the modal testing and model updating based on the correlation results is an important task during the development stage of the liquid rocket engine. These methods have been applied to rocket engines such as VINCI engine, RL10B-2, HM7B and the engine in China [1-4].

In this paper, an overview of the process of the modal testing and some results of updating the FE model through the correlation between the vibration modal testing results and the analysis results of the 75-ton class engine of the Korean Space Launch Vehicle II (KSLV-II) are presented.

2. Pre-test activities

2.1 Test planning

(1) Basic theories[5]

The modal testing is a test to identify a set of modal parameters of a test structure as mentioned before and the frequency response function(FRF) is used to identify modal parameters. FRF is a function used to qualify the response of the structure to an excitation force in the frequency domain and it is generally defined as:

$$H(\omega) = \frac{X(\omega)}{F(\omega)}$$

where

$F(\omega)$ is the input force spectrum,

$Y(\omega)$ is the output displacement spectrum.

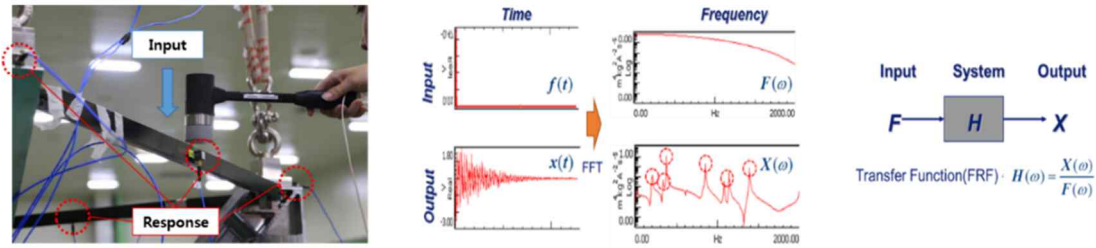


Figure 3: Concept of the modal testing and FRF

Modal parameters of the test structure and FE model are compared when updating the FE model. The mode pair table indicates the difference of the natural frequencies and the modal assurance criterion (MAC) indicates the difference of the mode shapes. Here, the MAC is a degree of correlation between two mode shapes and is defined as:

$$MAC = \frac{[\{\Phi_r\}^T \{\Phi_s\}]^2}{[\{\Phi_r\}^T \{\Phi_r\}][\{\Phi_s\}^T \{\Phi_s\}]}$$

where $\{\Phi_r\}$ and $\{\Phi_s\}$ are the two mode shapes

MAC = 1 indicates perfect correlation of the two mode shapes and MAC = 0 indicates no correlation of the two mode shapes.

Cross-orthogonality is another criterion to evaluate model correlation by checking the linear independence of a set of the test and analytical mode shapes using the mass matrix of the mathematical model as a weighting factor.

$$COC_{rs} = \frac{\{\Phi\}_{r,j}^T [M] \{\Phi\}_{s,j}}{\sqrt{\{\Phi\}_{r,j}^T [M] \{\Phi\}_{r,j}} \sqrt{\{\Phi\}_{s,k}^T [M] \{\Phi\}_{s,k}}}$$

where j and k are the two different sets of mode shaped (analytical and measured, respectively)

(2) Test plan

Since the rocket engine is a system composed of many components and the modal parameters of the system include the modal characteristics of the components, it is difficult to validate the modal characteristics of each component through the modal testing of the whole system at once and to classify and update the parameters of the FE model that cause the correlation differences. That is the reason a complicated system needs to be divided into the components and the FE model of the system needs to be updated with the modal parameters of each component. In this study, three sequential phases of the test, correlation and model updating were planned:

- phase 1. modal testing, correlation and model updating at the component level
- phase 2. modal testing, correlation and model updating at the subassembly level
- phase 3. modal testing, correlation and model updating at the complete engine level

A total of 31 steps of modal testing was planned at the component level including a combustion chamber, a turbo pump, high pressure pipelines, a gas generator, a turbine exhaust duct, a thrust frame, solenoid valve panel, harness panel, etc. After the modal testing of the components, engine assembly began and a total of 11 steps of modal testing at subassembly level and the completely assembled engine level were planned sequentially. Figure 4 shows conceptual diagram of the modal testing and model updating plan.

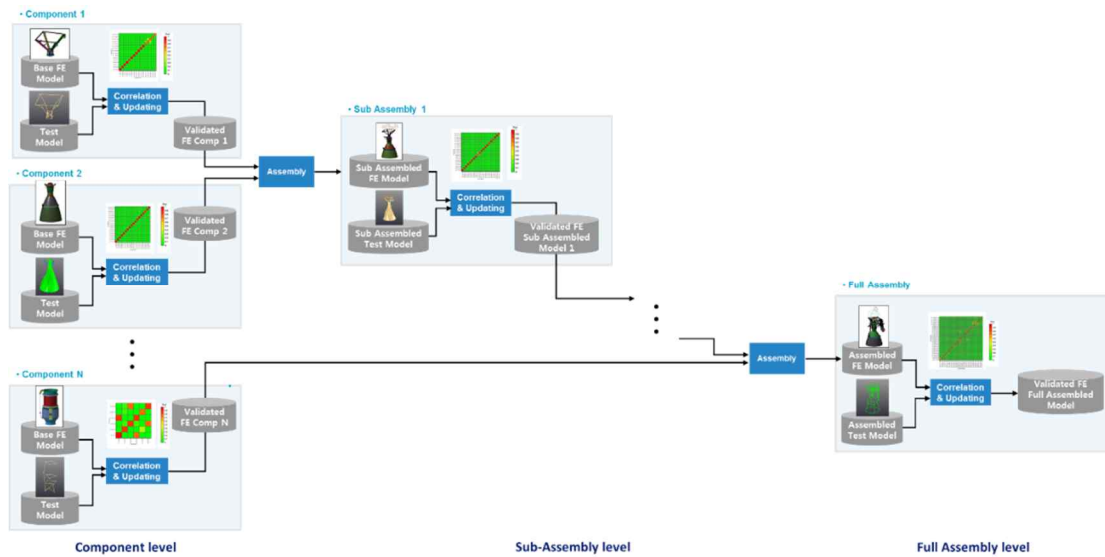


Figure 4: Conceptual diagram of the modal testing and model updating plan

2.2 Test setup

To perform the modal testing, test setup has to be prepared. The boundary conditions of each test structure have to be defined and applied. Methods and the locations of the excitation as an input and the locations and a number of accelerometers as an output need to be defined and installed on the test structure. Accelerometers and force transducers will be connected to the front-end device for data acquisition and the front-end device will be connected to PC where an advanced analysis software is installed for analysing the measured data.

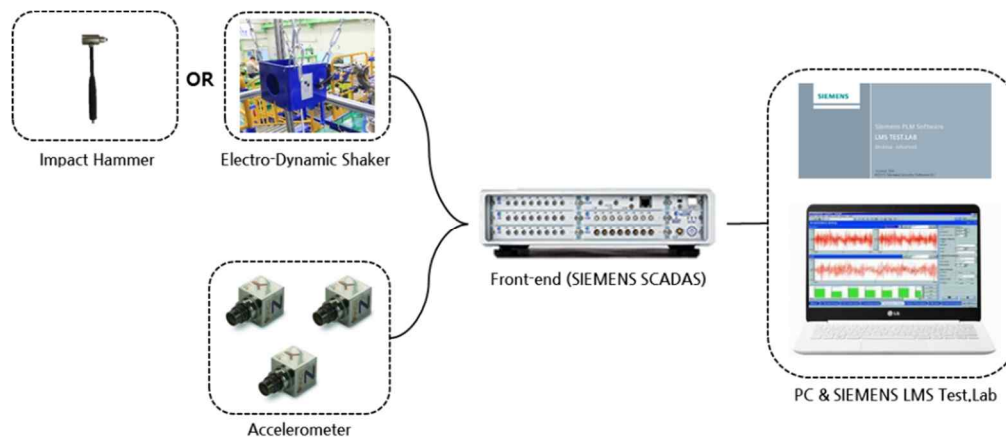


Figure 5: Test setup for the modal testing

The specific test setup applied in this study is as follows.

(1) Boundary conditions

If the test structure is freely floated in the air when performing the modal testing, the flexible modes of the structure can be clearly measured without affected by its boundary. However, it is not practical to float the test structure completely in the air. In reality, free-free conditions are implemented by hanging the test structure from elastic springs, bungee cords, etc. or by supporting it to flexible cushions such as sponges or air dampers. The method of the boundary condition should be decided so that it is sufficiently soft and the boundary condition has negligible effect on the flexible modes of the test structure. In this study, bungee cords were used for free-free boundary conditions and details of the cords were selected according to the rigid body mode measurement at test system check-out process. Details of the rigid body mode measurement will be summarized in 2.3(3).



Figure 6: Boundary conditions

(2) Force transducers

The impact hammer or the electro-dynamic shaker is generally used as an excitation instrumentation in the modal testing. Since impact hammer can excite the test structure at wide range of the frequencies with a single impulse, it is possible to perform a quick test using the impact hammer. However, since the impact hammer is the way the person is hand-held, it is difficult to control the magnitude of the excitation force and to examine the input dependency of the structure. On the other hands, the electro-dynamic shaker has the advantage of being able to examine the input dependency by applying various controlled excitation forces and measuring the responses to each excitation force. Its magnitude and frequency band of the excitation force are limited according to the specification of the shaker. It takes time to install and perform the modal testing compared with testing using the impact hammer.

In this study, the excitation using the impact hammer is applied at the component level and the subassembly level and both the impact hammer and electro-dynamic shaker are applied at the complete engine level. The excitation points of each test structure were determined to be enough to excite all modes within the frequency range of interest using the driving point survey which will be explained in 2.3(5). Figure 7 shows the setup of the electro-dynamic shakers at three points for the excitation of the complete engine.



Figure 7: Excitation setup using the electro-dynamic shaker

(3) Accelerometers

Accelerometers are installed to measure the response of the excitation. The type of the accelerometer is selected considering capacity of the frequency range, sensitivity, the mass loading effect, etc. The accelerometer should be installed in a position that can show all of the modes within the frequency range of interest. In this study, PCB miniature type tri-axial accelerometer was applied and pre-test analysis was conducted to demonstrate candidate sensor locations to accurately map the structural response of interest. A first choice for the points where the accelerometers are to be installed were selected according to the modal analyses of the FE models of each test structure and the adequacy of the selected locations was evaluated through the auto-MAC which is a criterion to compare a set of modes with themselves [6, 7].

If the auto-MAC shows high off-diagonal terms, it means the lack of the accelerometer leads to spatial aliasing and modification of the sensor locations or assignment of the additional sensors is necessary. The quantity and the locations of the accelerometers were finally determined so that the off-diagonal terms of the auto-MAC matrix were close to zero using the function of the maximum off-diagonal MAC analysis which is the pre-test analysis algorithm of Siemens LMS Virtual.Lab. Figure 8 shows accelerometer locations of the subassembly step 6, composed of the combustion chamber, gimbal mount, thrust frame, turbo pump, main valves, main pipelines, and their auto-MAC as an example.

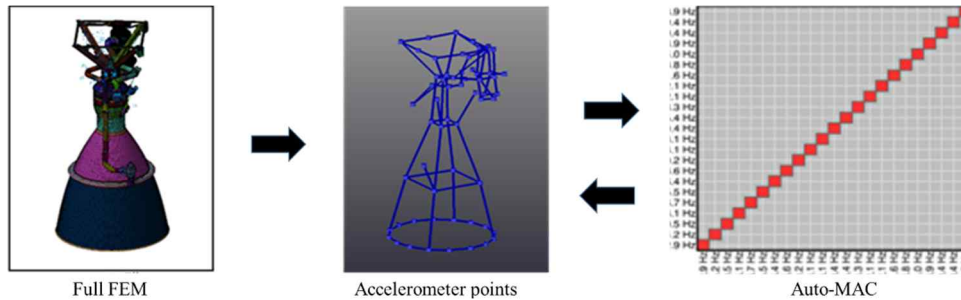


Figure 8: Accelerometer locations and auto-MAC of the subassembly step 6

(4) Data acquisition and analysis system

Siemens SCADAS Mobile and SCADAS Recorder as a data acquisition device were applied to measure input and output signals. Total six front-end modules were used which is available to measure maximum 320 channels of signals. Siemens LMS Test.Lab was used to analyze the measured data and PolyMAX, an advanced curve fitting algorithm of Test.Lab, was used to extract the modal parameters from the measured data [8].

2.3 Test system check-out

After the test setup, several check-outs of the test system were performed to improve the quality of the data measurement before the tests of each step. An ambient noise check, a rigid body mode check, a reciprocity check and an excitation point survey are included. The purpose and details of each check-out are as follows.

(1) Ambient noise check

An ambient noise check is a test to determine the ambient noise level of the test site and to verify the suitability of the environment by analyzing the signal to noise ratio. A comparison of the ambient and modal test data will determine the effect of the ambient noise on the test results and, if necessary, the noise source of the test site will be eliminated or reduced. In this study it was found that the ambient noise level was very low and did not affect the test.

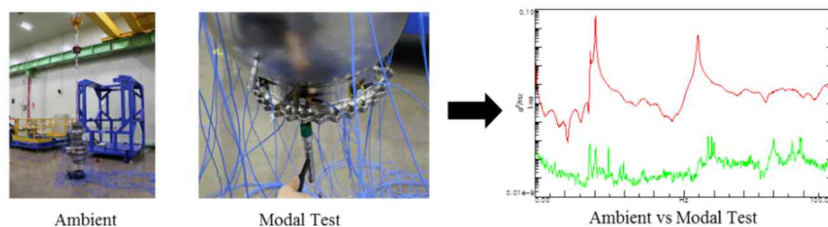


Figure 9: Ambient noise check

(2) Rigid body mode check

When the free-free boundary conditions are simulated using bungee cords, the rigid body mode has a non-zero value and if the bungee cords are stiff, the first flexible mode of the test structure will be coupled with the rigid body mode. It is advisable to separate the rigid body mode from the first flexible mode by applying the bungee cords as soft as possible within the height limit of the test site. Suitability of the boundary condition was estimated by shaking the test object hanging from the bungee cords up and down and verifying that the rigid body modes are less than 10 ~ 20 % of the first natural frequency of the test object. In this study, all of the rigid body modes of the components were less than 10 % and all of the subassemblies and complete engine were less than 20 % of the first natural frequency.

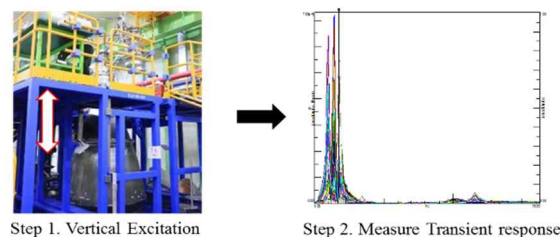


Figure 10: Rigid body mode check

(3) Reciprocity check

The mode test is a theory that is used under the assumption that the system is linear. Reciprocity is an indicator of the system linearity. Reciprocity means that the frequency response function H_{xy} , measured at x with excitation at y , is equal to the frequency response function H_{yx} , measured at y with excitation at x , if the system is exactly linear. In reality, however, H_{xy} and H_{yx} are not exactly equal due to the nonlinear elements of the test structure, the mass of the mounted transducer, the stiffening effects of the stringer and shaker, etc. [9] Most of the test structures showed the satisfactory reciprocity but several structures with bearings such as a gimbal mount, flexible bellows at the pipelines showed a little bit low reciprocity.

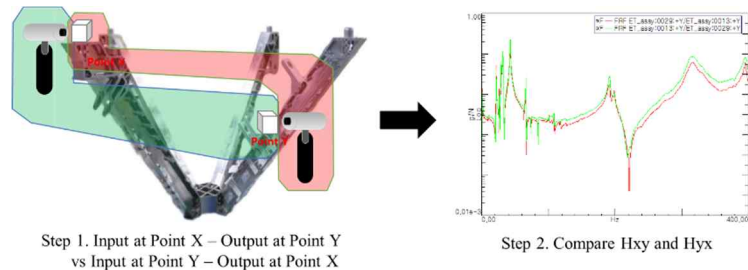


Figure 11: Reciprocity check of the thrust frame

(4) Driving point survey

A driving point survey is the process to select the optimal location for the excitation that can represent all modes of interest. A driving point measurement is to excite the force input at a point and measure the response at the same point and its FRF shows which modes are excited by the force input at that point. Since the rocket engine and its components are complex and huge structures, a number of the driving points necessary to excite all modes of interests were selected by performing the driving point survey.

3. The modal testing and model updating

3.1 Component level

(1) Modal testing

The modal tests of the components were carried out for about a month before the beginning of the assembly process. The modal tests on major components such as a combustion chamber, turbo pump, high-pressure pipes, turbine exhaust duct, thrust frame, etc. were conducted. Components expected to have characteristics of high natural frequencies beyond the frequency range of interest due to their small volume and high stiffness were reflected as point masses instead of performing the modal testing.

The thrust frame which is located between the gimbal mount of the engine and the rear fuselage is one of the good cases to review the process and the result of the component level modal testing. The tri-axial accelerometers were installed at 28 points decided by the pre-test analysis as shown in figure 12 and a total of 85 channels including 1 channel for the impact hammer was set for the testing. Free-free boundary conditions were implemented with bungee cords such that the rigid body mode was about 9% of the first natural frequency of the thrust frame.

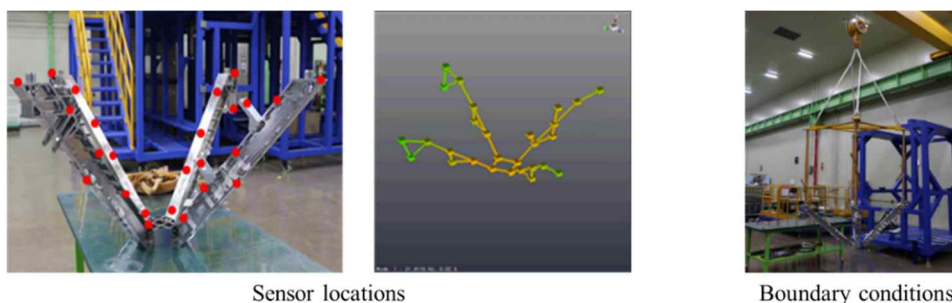


Figure 12: Test setup of the thrust frame

The test result showed that a number of natural frequencies and modal vectors were within the frequency range of interest. Figure 13 is the shape of the global bending mode, global torsion mode, and local torsion mode of the thrust frame and these modal parameters are to be used as a reference for the correlation and model updating.

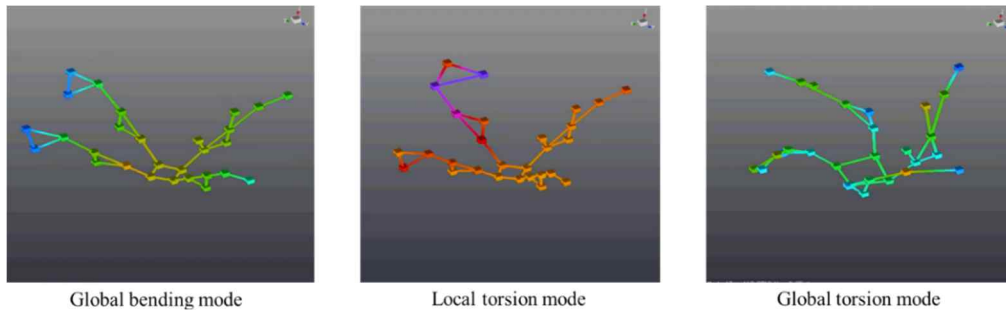


Figure 13: Mode shapes of the thrust frame

(2) Correlations and model updates

The model updating is generally achieved by modifying geometry, material properties, connection properties, etc. according to the correlation of the following parameters:

- mass
- natural frequencies (mode pair table)
- modal vectors (MAC matrix)

After the completion of the component level modal testing, the accuracies of the FE models were evaluated by the correlation between the test results and the analysis results for each component, and an iterative process was carried out for updating the FE model.

For the thrust frame, it was first found that the mass of the FE model was 1.2% higher than the test structure. The geometry of some simplified parts was adjusted and the material properties were modified to reduce the mass difference (update1). The results in table 1 showed that the frequency difference between the test and analysis results was significantly reduced from 32 ~ 57 % before the model updating to 3.9 ~ 11.1 % after the update 1. The model was additionally updated by modifying the connection properties of four thrust frames and the elastic modulus of materials (update 2). As a result of update 2, the natural frequency difference was reduced to 1.5 ~ 4.7.

Table 1: Difference of natural frequencies between test and analysis [%] of the thrust frame

	Before update	Update 1	Update 2
1	-32.0	-11.1	-4.7
2	-35.5	-8.9	-2.3
3	-33.1	-10.1	-3.6
4	-56.2	-3.9	3.0
5	-57.0	-5.4	1.5

Figure 14 and table 2 showed the MAC matrix of the thrust frame and its diagonal values, respectively. Diagonal values of MAC matrix were 0.457~0.867 originally and became 0.962~0.990, almost 1, after the model updating while the off diagonal term of MAC became almost 0. The results mean that the FE model was significantly improved and that modal parameters of the updated FE model and the test structure are in very good correlation.

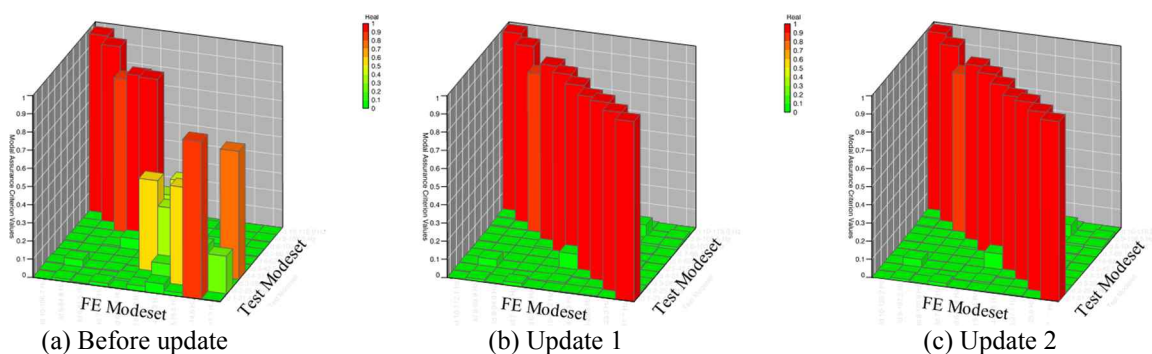


Figure 14: MAC matrix of the thrust frame

Table 2: Diagonal values of MAC at the thrust frame

	Before update	Update 1	Update 2
1	0.867	0.990	0.990
2	0.558	0.987	0.987
3	0.530	0.987	0.987
4	0.705	0.962	0.962
5	0.457	0.972	0.972

3.2 Sub-assembly and complete engine level

(1) Modal testing

After completing the modal testing of components, the engine was assembled according to the assembly process and the tests were performed at the subassembly and complete engine level. A total of 11 steps of subassemblies and the complete engine were tested during assembly process.

For a complete engine, the tri-axial accelerometers were installed at 81 points, equal to 243 channels, as shown in figure 15. The rigid body mode was about 18% of the first natural frequency of the engine system. Bungee cords needed to be more soft to decrease the ratio of rigid body mode to first flexible mode, but it had the limit to decrease the frequency of the rigid body mode since the height of the test site was limited. Instead, the boundary condition of the FE model was supplemented so that the analytical rigid body modes were not at 0 Hz but similar to the tested rigid body modes.



Figure 15: Test setup of the complete engine

A total of 37 natural frequencies and modes within the frequency range of interest were identified through the analysis of the test data and these included not only the global modes of the engine bending, engine torsion, combustion chamber oval, etc. but also the local modes of the tube lines, flexible bellows in turbine exhaust duct, solenoid valve panel, harness panel, etc. Figure 16 showed the shapes of the global bending mode, global torsion mode, the oval mode of the combustion chamber nozzle and the turbine exhaust duct and the local mode of the bellows.

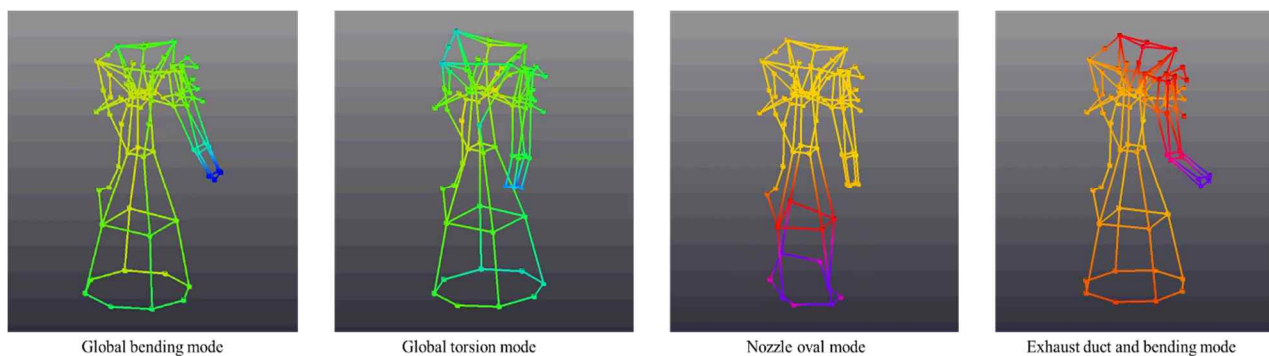


Figure 16: Mode shapes of the complete engine

(2) Correlation and model updating

Correlation and model updating of the FE models were performed based on the test results at the subassembly and complete assembly level. Since the FE models of the components have been already updated, the model updating of the subassemblies and the complete engine was achieved by mainly modifying the connection properties.

For the complete engine, all of the differences of the natural frequency within the frequency range of interest except 5 and 6 in second column of the table 3 which were the local modes of the turbine exhaust duct were less than 5 %. Figure 17 showed the 2D and 3D MAC matrix between the test modesets and the FE modesets of the updated engine model and third column of the table 3 indicated the diagonal values of MAC. All modes with high effective masses within the frequency range of interest showed the diagonal MAC values over 0.9. Most of the off-diagonal terms of the MAC were under 0.2. Some of the off-diagonal terms with the high value were considered as the effect of the lack of the accelerometers mostly at the components such as tube lines, flexible bellows at the turbine exhaust duct, panels, etc. which were expected to have low effective masses and the effect of the local modes of these components coupled with other fundamental modes. The way to separate these coupled modes so that off-diagonal terms are reduced close to zero is to add more accelerometers, but the quantity of the available accelerometers and channels of the front-end module are limited. Instead, the further study on the cross-orthogonality will be performed since it is the modal response weighted by the mass matrix and it will eliminate the effects of the local modal response of the components with low effective masses [10, 11].

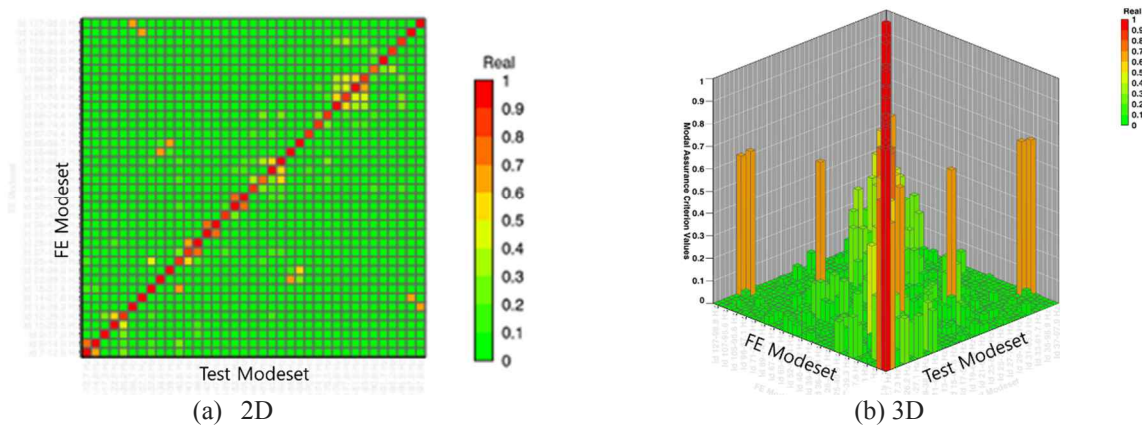


Figure 17: MAC matrix of the complete engine

Table 3: Results of the model updating of the complete engine

	Frequency difference [%]	Diagonal values of MAC
1	1.2	0.986
2	0.8	0.907
3	2.7	0.967
4	2.9	0.975
5	8.0	0.843
6	6.1	0.996
7	1.7	0.994
8	-4.3	0.977
9	1.8	0.978

4. Conclusions

During the development process of the KSLV-II engine, the vibration modal testing and the FE model updating based on the correlation of the test and analysis results were performed. Three phases of the test, the component level, the subassembly level, and the complete engine level were conducted to subdivide the modal parameters of the complete engine into the parameters of the components and to improve the accuracy of the correlation and the model updating. 31 steps for the components, 11 steps for the subassemblies and a test for the complete engine were conducted. The

modal parameters including natural frequencies, mode shapes, modal dampings of the engine and its components were defined by the modal testing. Correlations of the modal parameters obtained by the modal testing and the FE analysis were performed. The FE models were updated by modifying the geometries, material properties, connection properties, etc. and as a result the reliable FE models of the engine, its subassemblies and components were obtained. As well as the results of the test and model updating themselves, this project was meaningful in that the modal testing methods and procedures for a liquid rocket engine were established since it was the first vibration modal testing conducted for the liquid rocket engine in South Korea.

References

- [1] A. Sternchuss, A. Bossaert, P. Manfredi, N. David, and P. Alliot. 2014. The VINCI engine vibration test campaign. *50th AIAA/ASME/SAE/ASEE Joint Propulsion Conference*. AIAA 2014-3479
- [2] Pichon, T., Lacombe, A., Joyez, P., Ellis, R., Humbert, S., and Payne, M. 2001. *RL10B-2- nozzle extension assembly improvements for Delta IV*. AIAA 2001-3549,
- [3] Lekeux, A., Pander, J.P., and Mansouri, J. 2009. From qualification to 4th year of exploitation: HM7B on Ariane 5 ECA. *45th AIAA/ASME/SAE /ASEE Joint Propulsion Conference & Exhibit*. AIAA 2009-5036
- [4] Song Y., Bin L., Feng L., and Binchao L. 2017. Finite element model updating of liquid rocket engine nozzle based on modal test results obtained from 3-D SLDV technique. *Aerospace Science and Technology* 69. 412-418
- [5] ESA publication division. 2005. Space engineering : modal survey assessment. *European Cooperation for Space Standardization*
- [6] D. J. Edwins. 2000. Modal testing, theory, practice, and application 2nd ed. *Research Study Press Ltd*.
- [7] Andreas, Optimal sensor placement for modal testing on wind turbines. *Journal of Physics Conference Series* 753 (2016) 072031
- [8] Bart P., Herman V., Patrick G. and Jan L. 2004. The PolyMAX frequency-domain method: a new standard for modal parameter estimation? *Shock and Vibration* 11. 395-409
- [9] Peter A. 2017. Modal testing : a practitioner's guide, *John Wiley & Sons*
- [10] Mark E. M., Thomas W. G., Kelly S. C., and Kim D. O. 2002. Lessons learned from CM-2 modal testing and analysis. *NASA/TM-2002-211692*
- [11] Rnadall J. A. 2003. The modal assurance criterion – twenty years of use and abuse. *Sound and Vibration*